

Modeling Frequency and Severity of Claims with the Generalized Cluster-Weighted Model

Nikola Počuča, Tatjana Miljkovic, Petar Jevtić, Paul McNicholas

August 31, 2018

Abstract

In this paper, we propose a generalized cluster-weighted model (GCWM) that allows for modeling non-Gaussian distribution of the continuous covariates and a new zero-inflated GCWM (ZI-GCWM) for modeling insurance claims data with excess zeros. We describe two expectation-optimization (EM) algorithms for parameter estimation in GCWM and ZI-GCWM. A simulation study showed that both cluster models perform well for different settings in contrast to the existing mixture-based approaches. A real data set based on French automobile policies is used to illustrate the application of the proposed models.

KEY WORDS: GCWM, CWM, ZI-GCWM, clustering, automobile claims.

JEL CLASSIFICATION: C02, C40, C60.

1 Introduction

A significant number of clustering methods have been proposed for sub-grouping the data in the area of computer science, biology, social science, statistics, marketing, etc. Ingrassia and Minotti (2015) proposed a cluster-weighted models (CWMs) as a flexible family of mixture models for fitting the joint distribution of a random vector composed of a response variable and a set of mixed-type covariates with the assumption that continuous covariates come from Gaussian distribution. The CWM models with Gaussian assumptions have been proposed by Gershenfeld (1997), Gershenfeld and Metois (1999), and Gershenfeld (1999) in a context of media technology. Some extensions of this class of models have been considered by Punzo and Ingrassia (2014), Ingrassia and Punzo (2014), and Ingrassia and Vittadini (2014). These clustering methods lack some capabilities

in order to be able to accommodate modeling insurance data (e.g. high excess zeros for claim count, heavy-tail loss distribution, deductible, or limits).

Sub-grouping of insurance policies based on risk classification is a standard practice in insurance. The heterogeneous nature of insurance data allows for explorations of many different techniques for sub-grouping risk. As a result, there is a growing number of papers in the area of mixture modeling of univariate and multivariate insurance data to account for heterogeneity of risk. Lee and Lin (2010), Verbelen et al. (2015), and Miljkovic and Grün (2016) proposed mixture models for univariate loss data. The idea of mixture modeling of univariate insurance data has been extended to a multivariate classification. A finite mixture of bivariate Poisson regression models with an application to insurance ratemaking was studied by Bermúdez and Karlis (2012). A Poisson mixture model for count data was considered by Brown and Buckley (2015) with application in managing Group Life insurance portfolio. Miljkovic and Fernández (2018) reviewed two complementary mixture-based clustering approaches (cluster-weighted model and mixture-based clustering for an ordered stereotype model) for modeling unobserved heterogeneity in an automobile insurance portfolio, depending on the data structure under consideration. Mixture models with the applications in financial mathematics have been explored by Durham (2007), Miljkovic and SenGupta (2018), and many others.

In this paper, we extend the CWM family proposed by Ingrassia and Minotti (2015) to allow for modeling of non-Gaussian continuous covariates and a zero-inflated Poisson (ZIP) claims data with excess zeros which are commonly seen in the insurance applications. We define our proposed model as the generalized cluster-weighted model as GCWM and a new zero-inflated GCWM as ZI-GCWM. Two partitioning methods are considered with two separate EM algorithms. The first EM algorithm is for generating the GCWM models, while the second EM is for optimizing the ZI-GCWM. We show that the Bernoulli and Poisson GCWM accurately estimate the initialization of the EM algorithm for the ZI-GCWM model. These models utilize individual policy and claims data and should be useful in the areas of ratemaking and risk management.

This paper is organized as follows. Section 2 presents the proposed model for mixture of GLMs. Section 3 develops and discusses estimation methodology. Section 4 Applies the proposed model on a real data of French automobile claims, in addition an extensive simulation study is discussed. Conclusion is provided in Section 5.

2 Model

2.1 Background

Let $(\mathbf{X}', Y)'$ be the pair of a vector of covariates \mathbf{X} and a response variable Y . Assume this set is defined on some sample space Ω that takes values in an appropriate Euclidian subspace. Now, assume that there exists G partitions of Ω , denoted as $\Omega_1, \dots, \Omega_G$. Gershenfeld (1997) characterized the cluster-weighted models as a finite mixture of GLMs hence, the joint distribution $f(\mathbf{x}, y)$ of $(\mathbf{X}', Y)'$ is expressed as follows

$$f(\mathbf{x}, y) = \sum_{j=1}^G \tau_j q(y|\mathbf{x}; \Omega_j) p(\mathbf{x}; \Omega_j). \quad (2.1)$$

The pair $q(y|\mathbf{x}; \Omega_j)$ and $p(\mathbf{x}; \Omega_j)$ are conditional and marginal distributions of $(\mathbf{X}', Y)'$ respectively, while τ_j represents the weight of the j th component such that $\sum_{j=1}^G \tau_j = 1$, $\tau_j > 0$. Ingrassia and Minotti (2015) proposed a flexible family of mixture models for fitting the joint distribution of a random vector $(\mathbf{X}', Y)'$ by splitting the covariates into continues and discrete as $\mathbf{X} = (\mathbf{V}', \mathbf{W}')'$. This assumption of independence between continues and discrete covariates allows us to multiply their corresponding marginal distributions. Thus, for this setting the model in (2.1) is reformulated as follows

$$f(\mathbf{x}, y; \Phi) = \sum_{j=1}^G \tau_j q(y|\mathbf{x}; \boldsymbol{\vartheta}_j) p(\mathbf{x}; \boldsymbol{\theta}_j) = \sum_{j=1}^G \tau_j q(y|\mathbf{x}; \boldsymbol{\vartheta}_j) p(\mathbf{v}; \boldsymbol{\theta}_j^*) p(\mathbf{w}; \boldsymbol{\theta}_j^{**}) \quad (2.2)$$

where \mathbf{v} and \mathbf{w} are the vectors of continues and discrete covariates respectively, the $q(y|\mathbf{x}; \boldsymbol{\vartheta}_j)$ is the conditional density of $Y|\mathbf{x}$, with parameter vector $\boldsymbol{\vartheta}_j$, the $p(\mathbf{v}; \boldsymbol{\theta}_j^*)$ is the marginal distribution of \mathbf{v} with parameter vector $\boldsymbol{\theta}_j^*$. the $p(\mathbf{w}; \boldsymbol{\theta}_j^{**})$ is the marginal distribution of \mathbf{w} with parameter vector $\boldsymbol{\theta}_j^{**}$. Finally, $\Phi := (\boldsymbol{\theta}^*, \boldsymbol{\theta}^{**}, \boldsymbol{\tau}, \boldsymbol{\vartheta})$ includes all model parameters. In addition, the conditional distribution $q(y|\mathbf{x}; \boldsymbol{\vartheta}_j)$ is assumed to belong to an exponential family of distributions and as such can be modeled in the framework of GLMs. Here, the marginal distribution of continues covariates is assumed to be of Gaussian type. Unfortunately, this last assumption is too strong for use in insurance related applications specifically in rate-making. To relax it, we develop the Generalized cluster-weighted mdoel (GCWM) that allows for non-Gaussian covariates as discussed in the next section.

2.2 Generalized cluster-weighted model (GCWM)

We proceed to extend (2.2) by splitting the continuous covariates further as $\mathbf{V} := (\mathbf{U}', \mathbf{T}')'$, where \mathbf{U} is a set of non-Gaussian covariates, and \mathbf{T} a set of Gaussian covariates. Thus (2.2) is now recovered as

$$f(\mathbf{x}, y; \Phi) = \sum_{j=1}^G \tau_j q(y|\mathbf{x}; \boldsymbol{\vartheta}_j) p(\mathbf{t}; \boldsymbol{\theta}_j^*) p(\mathbf{w}; \boldsymbol{\theta}_j^{**}) p(\mathbf{u}; \boldsymbol{\theta}_j^{***}) \quad (2.3)$$

which we refer to as generalized cluster-weighted model (GCWM). Here $p(\mathbf{t}; \boldsymbol{\theta}_j^*)$ denotes the marginal density of Gaussian covariates, with parameter vector $\boldsymbol{\theta}^*$, and $p(\mathbf{u}; \boldsymbol{\theta}_j^{***})$ as the marginal density of the non-Gaussian covariates with parameter vector $\boldsymbol{\theta}_j^{***}$.

As it is relevant to the actuarial application in this paper, we focus on the multivariate log-normal distribution for non-Gaussian covariates. This however does not reduce the generality of our approach. With log-normal assumption for $p(\mathbf{u}; \boldsymbol{\theta}_j^{***})$ we have that \mathbf{u} is defined on \mathbb{R}_+^p , $p \in \mathcal{N}$ with parameter vector $\boldsymbol{\theta}_j^{***}$ having probability density function as

$$p(\mathbf{u}; \boldsymbol{\theta}_j^{***} := (\boldsymbol{\mu}_j^{***}, \boldsymbol{\Sigma}_j^{***})) = \frac{1}{(\prod_{i=1}^p u_i) |\boldsymbol{\Sigma}_j^{***}| (2\pi)^{\frac{p}{2}}} \exp \left[-\frac{1}{2} (\ln \mathbf{u} - \boldsymbol{\mu}_j^{***})' \boldsymbol{\Sigma}_j^{***-1} (\ln \mathbf{u} - \boldsymbol{\mu}_j^{***}) \right].$$

The derivation of the equation above can be found in the Appendix 7.1.

2.3 Zero-inflated Poisson Model

In the zero-inflated Poisson model (ZIP) (see Lambert (1992)) we can split the conditional density $p(y|\mathbf{x}, \boldsymbol{\vartheta}_j)$ of the response variable y , into zero and non-zero densities. The conditional probability mass associated with the event $y = 0$ is characterized with function $q(y = 0|\mathbf{x}, \boldsymbol{\vartheta}_j)$. For situations when $y > 0$ the response variable y is conditionally distributed with density $q(y > 0|\mathbf{x}, \boldsymbol{\vartheta}_j)$. Given the conditional density now defined for the ZIP model (2.3) can be re-written as follows

$$f(\mathbf{x}, y; \Phi) = \sum_{j=1}^G \tau_j [q(y = 0|\mathbf{x}; \boldsymbol{\vartheta}_j) + q(y > 0|\mathbf{x}; \boldsymbol{\vartheta}_j)] p(\mathbf{t}; \boldsymbol{\theta}_j^*) p(\mathbf{w}; \boldsymbol{\theta}_j^{**}) p(\mathbf{u}; \boldsymbol{\theta}_j^{***}). \quad (2.4)$$

Let $\tilde{\mathbf{x}} := [1, \mathbf{x}]$, where $\tilde{\mathbf{x}}$ is a matrix of covariates with the addition of a placeholder for the intercept in the GLM. We denote the Poisson conditional density as $q^P(y|\mathbf{x}; \lambda_j)$, where $y \in \{0, 1, \dots\}$, and β_j is a row coefficient vector. Here, the link function will be modelled with log-link for the GLM such that

$$\lambda_j = e^{\tilde{\mathbf{x}}\beta_j'} \quad \text{and} \quad q^P(y|\mathbf{x}; \lambda_j) = e^{-\lambda_j} \frac{\lambda_j^y}{y!}.$$

Next, we introduce a Bernoulli model for the conditional density. We denote the density as $q^B(y|\mathbf{x}; \bar{\beta}_j)$, where

$\bar{\beta}_j$ is a row coefficient vector. Here, the GLM will be modeled with the associated logit link function such that

$$\psi_j = \frac{e^{\tilde{\mathbf{x}}\bar{\beta}_j'}}{1 + e^{\tilde{\mathbf{x}}\bar{\beta}_j'}} \quad \text{and} \quad q^B(y|\mathbf{x}; \psi_j) = \begin{cases} \psi_j, & y = 0 \\ 1 - \psi_j, & y = 1 \end{cases}$$

Now, given a combination of two preceding models, we introduce the zero inflated Poisson model in which zero counts come from two random variables. One comes from Bernoulli random variable which generates structural zeros, and the other comes from the Poisson random variable. The coefficients pair $\{\beta_j, \bar{\beta}_j\} := \boldsymbol{\vartheta}_j$ correspond to the two above introduced conditional densities where the coefficients are estimated using a generalized linear model as in Lambert (1992). The components of ZIP conditional density $q(y|\mathbf{x}; \boldsymbol{\vartheta}_j)$ are

$$q(y = 0|\mathbf{x}; \boldsymbol{\vartheta}_j) = \psi_j + (1 - \psi_j)e^{-\lambda_j} \quad \text{and} \quad q(y > 0|\mathbf{x}; \boldsymbol{\vartheta}_j) = (1 - \psi_j)e^{-\lambda_j} \frac{(\lambda_j)^y}{y!}.$$

Also, the link functions to consider are log-link for the Poisson and logit link for the Bernoulli model such that

$$\psi_j = \frac{e^{\tilde{\mathbf{x}}\bar{\beta}_j'}}{1 + e^{\tilde{\mathbf{x}}\bar{\beta}_j'}} \quad \text{and} \quad \lambda_j = e^{\tilde{\mathbf{x}}\beta_j'}.$$

Let parameter ψ_j denote the probability that the zero comes from the Bernoulli distribution of j th component, and the parameter λ_j characterizes the j th Poisson distribution. This allows for a more nuanced approach to handling the inflation of zeros for automobile insurance (see Bermúdez and Karlis (2012)).

2.4 Bernoulli-Poisson Sample Space Partitioning

The single component ZIP model assumes that the inflated zeros emanate from both a Bernoulli and Poisson random variables while the non-zeros are assumed to come exclusively from the Poisson random variable. However, recent research extends the single component ZIP models to mixture models for heterogeneous count data with excess zeros (see Bermúdez and Karlis (2012)). In mixtures of ZIPs, zeros are assumed to come from multiple different Binomial and Poisson random variables. Difficulties are apparent during the maximization step of the EM when means of covariates are very close together (see Lim et al. (2014)). However, misclassification error can be reduced using parsimonious models for the independent variables as in McNicholas et al. (2010).

In this work, we propose a new method to rectify this problem and partition the dataset using Bernoulli and Poisson GCWMs. Furthermore, we construct a new zero inflated GCWM (ZI-GCWM) using the previously generated Bernoulli and Poisson GCWMs. We show that the Bernoulli and Poisson GCWM accurately estimate the initialization of the EM algorithm for the zero inflated GCWM model. The work of Lambert (1992) specifies that the MLE estimates for coefficients provide an excellent guess allowing EM to converge quickly for ZIPs.

The partitioning method consists of two separate EM algorithms. The first EM algorithm is for generating the GCWM models, while the second EM is for optimizing the ZI-GCWM. Recall $(\mathbf{X}', Y)'$ to be a vector defined on some sample space Ω . As discussed, this sample space is partitioned into G non-overlapping sets such that their union constitutes this sample space ie. $\Omega = \bigcup_{i=1}^G \Omega_i$. However, contingent on a model choice each particular set Ω_i may take a different shape. Specifically, if we introduce the Bernoulli model in a generalized form for conditional density (see Ingrassia and Minotti (2015) for specific cases), we have the sample space Ω^B and joint probability density function f^B to be

$$\Omega^B = \bigcup_{l=1}^G \Omega_l^B \quad \text{and} \quad f^B(\mathbf{x}, y; \Phi) = \sum_{l=1}^G \tau_l q^B(y|\mathbf{x}; \bar{\beta}_l) p(\mathbf{t}; \boldsymbol{\theta}_l^*) p(\mathbf{w}; \boldsymbol{\theta}_l^{**}) p(\mathbf{u}; \boldsymbol{\theta}_l^{***}).$$

Similarly if we introduce a Poisson model in a generalized form the sample space Ω^P and joint probability density function f^P become

$$\Omega^P = \bigcup_{j=1}^M \Omega_j^P \quad \text{and} \quad f^P(\mathbf{x}, y; \Phi) = \sum_{j=1}^M \tau_j q^P(y|\mathbf{x}; \beta_j) p(\mathbf{t}; \boldsymbol{\theta}_j^*) p(\mathbf{w}; \boldsymbol{\theta}_j^{**}) p(\mathbf{u}; \boldsymbol{\theta}_j^{***}).$$

Where this sample space is partitioned up to M non-overlapping sets. Now, construct a new partitioning of a sample space Ω such that

$$\Omega = \Omega^Z = \bigcup_{\substack{l \in \{1, \dots, G\} \\ j \in \{1, \dots, M\}}} \Omega_{l,j}^Z := \bigcup_{\substack{l \in \{1, \dots, G\} \\ j \in \{1, \dots, M\}}} \Omega_l^B \cap \Omega_j^P =: \bigcup_{k \in \{1, \dots, K \leq M \times G\}} \Omega_k^Z,$$

where K can range up to $M \times G$ unique partitions. Therefore the new conditional density is now result of a model in which each component is captured by the conditional probability density function that is a mixture of particular Bernoulli and particular Poisson densities

$$\begin{aligned} q_k^Z(y|\mathbf{x}; \bar{\beta}_k, \beta_k) &:= q^B(y|\mathbf{x}; \bar{\beta}_k) + (1 - q^B(y|\mathbf{x}; \bar{\beta}_k)) q^P(y|\mathbf{x}; \beta_k) \\ &= q(y = 0|\mathbf{x}; \boldsymbol{\vartheta}_k) + q(y > 0|\mathbf{x}; \boldsymbol{\vartheta}_k), \quad k \in \{1, \dots, K\}. \end{aligned} \quad (2.5)$$

The expectation-maximization (EM) algorithm (see Dempster et al. (1977)) is then used to estimate this new mixture of up to $M \times G$ specific GCWMs. The initialization parameters for the second EM algorithm are provided by Bernoulli and Poisson GCWMs from (2.5) giving parameter pairs (ψ_k, λ_k) . The second EM procedure then optimizes (2.5). The ZI-GCWM is then compared against the standard Poisson GCWM using a likelihood ratio test which is commented in section 3.6.

3 Estimation Methodology

The common approach for estimating parameters in finite mixture problems is based on the EM algorithm (see McLachlan and Peel (2000)). The estimation of the developed Bernoulli-Poisson partitioning method is split into two EM algorithms. The first EM algorithm partitions the sample space, while the second EM algorithm optimizes the zero inflated portion.

3.1 The EM Algorithm for Partitioning of Sample Space

The EM algorithm is based on the local maximum likelihood estimation. The initial values of the parameter estimates can be generated from a variety of strategies outlined in Biernacki et al. (2000). The algorithm proceeds by alternation of the E-step and M-step to update parameter estimates. To find an optimal number of components, maximum likelihood estimation is obtained over a range of G groups, and the best model is selected based on the Bayesian information criterion (BIC).

The convergence criterion of the EM algorithm is based on the Aitken acceleration. It is used to estimate the asymptotic maximum of the log-likelihood at each iteration of the EM algorithm. when the relative increase in the log-likelihood function is no bigger than a small pre-specified tolerance value or the number of iterations reach a limit.

In this subsection, we explain the parameter estimation in line with the GCWM methodology proposed by Ingrassia and Minotti (2015). The proposed GCWM is based on the assumption that $q(y|\mathbf{x}, \boldsymbol{\vartheta}_j)$ belongs to the exponential family of distributions that are strictly related to GLMs. The link function defines the relationship between the linear predictor and the expected value of the distribution function as $g(\boldsymbol{\mu}_j) = \tilde{\mathbf{x}}\boldsymbol{\beta}'$, where $g(\boldsymbol{\mu}_j)$ is the link function. We are interested in the estimation of the vector $\boldsymbol{\beta}_j$, thus the distribution of $y|\mathbf{x}$ is denoted by $q(y|\mathbf{x}; \boldsymbol{\beta}_j, \lambda_j)$, where λ_j denotes an additional parameter to account for when a distribution belongs to a two-parameter exponential family.

The marginal distribution $p(\mathbf{x}; \boldsymbol{\theta}_j)$ has the following components: $p(\mathbf{t}; \boldsymbol{\theta}_j^*)$, $p(\mathbf{w}; \boldsymbol{\theta}_j^{**})$, and $p(\mathbf{u}; \boldsymbol{\theta}_j^{***})$. The first marginal density $p(\mathbf{t}; \boldsymbol{\theta}_j^*)$ is modeled as a Gaussian distribution with mean $\boldsymbol{\mu}_j^*$ and covariance matrix $\boldsymbol{\Sigma}_j^*$ hence $p(\mathbf{t}; \boldsymbol{\mu}_j^*, \boldsymbol{\Sigma}_j^*)$. When it comes to the second marginal density $p(\mathbf{w}; \boldsymbol{\theta}_j^{**})$, we assume that each finite discrete covariate W is represented as a vector $\mathbf{w}^r = (w^{r1}, \dots, w^{rc_r})'$ where $w^{rs} = 1$ if $w_r = s$, such that $s \in \{1, \dots, c_r\}$, and $w^{rs} = 0$ otherwise.

$$p(\mathbf{w}; \boldsymbol{\gamma}_j) = \prod_{r=1}^d \prod_{s=1}^{c_r} (\gamma_{jrs})^{w^{rs}} \quad (3.1)$$

for $j = 1, \dots, G$, where $\boldsymbol{\gamma}_j = (\gamma'_{j1}, \dots, \gamma'_{jd})'$, $\boldsymbol{\gamma}_{jr} = (\gamma'_{jr1}, \dots, \gamma'_{jrc_d})'$, $\gamma_{jrs} > 0$, and $\sum_{s=1}^{c_r} \gamma_{jrs}$, $r =$

$1, \dots, q$. The density $p(\mathbf{w}, \gamma_j)$ represents the product of d conditionally independent multinomial distributions with parameters γ_{jr} , $r = 1, \dots, d$. Finally, the third marginal density $p(\mathbf{u}; \theta_j^{***})$ will be modelled with a multivariate log-normal distribution having a location parameter vector $\boldsymbol{\mu}_j^{***}$ and scale parameter matrix $\boldsymbol{\Sigma}_j^{***}$.

Let $(\mathbf{x}_1, y_1), \dots, (\mathbf{x}_n, y_n)$ be a sample of n independent observations drawn from model in (2.3). For this sample, the complete data likelihood function, $L_c(\Phi)$, is given by

$$L_c(\Phi) = \prod_{i=1}^n \prod_{j=1}^G [\tau_j q(y_i | x_i; \beta_j, \lambda_j) p(t_i; \boldsymbol{\mu}_j^*, \boldsymbol{\Sigma}_j^*) p(w_i; \gamma_j) p(u_i; \boldsymbol{\mu}_j^{***}, \boldsymbol{\Sigma}_j^{***})]^{z_{ij}}, \quad (3.2)$$

where z_{ij} is the latent indicator variable with value of $z_{ij} = 1$ indicating that observation (\mathbf{x}_i, y_i) , originated from the j th mixture component and $z_{ij} = 0$ otherwise.

By taking the logarithm of (3.2), the complete-data log-likelihood function $\ell_c(\Phi)$ is written by

$$\begin{aligned} \ell_c(\Phi) = \sum_{i=1}^n \sum_{j=1}^G z_{ij} [& \log(\tau_j) + \log q(y_i | x_i; \beta_j, \lambda_j) + \\ & \log p(t_i; \boldsymbol{\mu}_j^*, \boldsymbol{\Sigma}_j^*) + \log p(w_i; \gamma_j) + \log p(u_i; \boldsymbol{\mu}_j^{***}, \boldsymbol{\Sigma}_j^{***})]. \end{aligned} \quad (3.3)$$

3.1.1 E-Step - Partitioning

The E -step in the $(s + 1)$ th iteration requires calculation of the conditional expectation of $\ell_c(\Phi)$. Since $\ell_c(\Phi)$ is linear with respect to z_{ij} , we simplify the calculation to the current expectation of Z_{ij} , where Z_{ij} is the random variable corresponding to z_{ij} . Given the previous parameters $\Phi^{(s)}$ and the observed data, we calculate the current conditional expectation of Z_{ij} as

$$\begin{aligned} \pi_{ij}^{(s)} &= E[Z_{ij} | (\mathbf{x}_i, y_i); \Phi^{(s)}] \\ &= \frac{\tau_j^{(s)} q(y_i | x_i; \beta_j^{(s)}, \lambda_j^{(s)}) p(t_i; \boldsymbol{\mu}_j^{*(s)}, \boldsymbol{\Sigma}_j^{*(s)}) p(w_i; \gamma_j^{(s)}) p(u_i; \boldsymbol{\mu}_j^{*** (s)}, \boldsymbol{\Sigma}_j^{*** (s)})}{f(\mathbf{x}_i, y_i; \Phi^{(s)})}. \end{aligned}$$

3.1.2 M-Step - Partitioning

In the M -step, given the $(s + 1)$ th iteration the conditional expectation of $\ell_c(\Phi)$ is maximized with respect to Φ . Let $Q(\Phi | \Phi^{(s)})$ be an intermediate maximization function on the $(s + 1)$ th iteration. The values of z_{ij} in (3.3) are replaced by their current expectations π_{ij} yielding

$$\begin{aligned}
Q(\Phi|\Phi^{(s)}) &= \sum_{i=1}^n \sum_{j=1}^G \pi_{ij}^{(s)} [\log(\tau_j) + \log q(y_i|x_i; \beta_j, \lambda_j) + \log p(t_i; \mu_j^*, \Sigma_j^*) + \log p(w_i; \gamma_j) + \log p(u_i; \mu_j^{***}, \Sigma_j^{***})] \\
&= \sum_{i=1}^n \sum_{j=1}^G \pi_{ij}^{(s)} \log(\tau_j) + \sum_{i=1}^n \sum_{j=1}^G \pi_{ij}^{(s)} \log q(y_i|x_i; \beta_j, \lambda_j) + \sum_{i=1}^n \sum_{j=1}^G \pi_{ij}^{(s)} \log p(t_i; \mu_j^*, \Sigma_j^*) \\
&\quad + \sum_{i=1}^n \sum_{j=1}^G \pi_{ij}^{(s)} \log p(w_i; \gamma_j) + \sum_{i=1}^n \sum_{j=1}^G \pi_{ij}^{(s)} \log p(u_i; \mu_j^{***}, \Sigma_j^{***}). \quad (3.4)
\end{aligned}$$

The M-step requires maximization of the Q -function with respect to Φ which can be done separately for each term on the right hand side in (3.4). As a result, the parameter updates $\hat{\tau}_j$, $\hat{\mu}_j^*$, $\hat{\Sigma}_j^*$, and $\hat{\gamma}_j$ on the $(s+1)$ th iteration are

$$\begin{aligned}
\hat{\tau}_j^{(s+1)} &= \frac{1}{n} \sum_{i=1}^n \pi_{ij}^{(s)}, & \hat{\mu}_j^{*(s+1)} &= \frac{1}{\sum_{i=1}^n \pi_{ij}^{(s)}} \sum_{i=1}^n \pi_{ij}^{(s)} t_i, & \hat{\gamma}_{jr}^{(s+1)} &= \frac{\sum_{i=1}^n \pi_{ij}^{(s)} \omega_i^{rs}}{\sum_{i=1}^n \pi_{ij}^{(s)}}, \\
\hat{\Sigma}_j^{*(s+1)} &= \frac{1}{\sum_{i=1}^n \pi_{ij}^{(s)}} \sum_{i=1}^n \pi_{ij}^{(s)} (t_i - \hat{\mu}_j^{*(s+1)})(t_i - \hat{\mu}_j^{*(s+1)})',
\end{aligned}$$

Parameter estimates for the log-normal distribution follow similar suit.

$$\hat{\mu}_j^{***(s+1)} = \frac{1}{\sum_{i=1}^n \pi_{ij}^{(s)}} \sum_{i=1}^n \pi_{ij}^{(s)} \ln u_i, \quad \hat{\Sigma}_j^{***(s+1)} = \frac{1}{\sum_{i=1}^n \pi_{ij}^{(s)}} \sum_{i=1}^n \pi_{ij}^{(s)} (\ln u_i - \hat{\mu}_j^{***(s+1)})(\ln u_i - \hat{\mu}_j^{***(s+1)})'.$$

The estimates of vector β are computed by maximizing each of the G terms

$$\sum_{i=1}^n \pi_{ij}^{(s)} \log q(y_i|x_i; \beta_j, \lambda_j). \quad (3.5)$$

Maximization of (3.5) is performed by numerical optimization in R software. A similar framework the mixture of generalized linear models are implemented. For additional details about this implementation the reader is refer to Wedel and De Sabro (1995) and Wedel (2002).

For insurance applications, current GCWM model can be used for modeling frequency of claims assuming that \mathbf{Y} belongs to Poisson or Bernoulli distributions. When modelling severity of claims, \mathbf{X} can be assumed accommodate Gamma or Log-normal distributions. All of these applications are based on CWM as the underlying approach. For additional implementation information, the reader is referred to the manual of the `flexCWM` package manual for R users written by Ingrassia and Minotti (2015).

3.2 EM Algorithm for Zero-inflated Model

The optimization of the zero-inflated Poisson model given in (2.5), uses the EM algorithm for maximizing the incomplete-data log-likelihood iteratively (see Lambert (1992)). The log-likelihood function of ψ_k and λ_k is expressed as

$$l(\psi_k, \lambda_k; y, \mathbf{x}) = \sum_{y_i=0} \log [e^{\tilde{\mathbf{x}}_i \tilde{\boldsymbol{\beta}}'_k} + \exp(-e^{\tilde{\mathbf{x}}_i \boldsymbol{\beta}'_k})] + \sum_{y_i>0} (y_i \tilde{\mathbf{x}}_i \boldsymbol{\beta}'_k + e^{\tilde{\mathbf{x}}_i \boldsymbol{\beta}'_k}) - \sum_{i=1}^n \log(1 + e^{\tilde{\mathbf{x}}_i \tilde{\boldsymbol{\beta}}'_k}) - \sum_{y_i>0} \log(y_i!)$$

Where y_i , and $\tilde{\mathbf{x}}_i$ refers to the i th row of the response variable y and covariate matrix $\tilde{\mathbf{x}}$. Due to the first term the log-likelihood function is rather complicated to maximize. However, Lambert (1992) gives a meaningful solution.

Suppose that we could observe $\mathcal{O}_{ik} = 1$ when y_i is generated from the Bernoulli random variable of partition k , and $\mathcal{O}_{ik} = 0$ when y_i is generated from the Poisson random variable. Then the complete-data log-likelihood would be written as

$$\begin{aligned} l_c(\psi_k, \lambda_k; y, \mathbf{x}, \mathbf{o}_k) &= \sum_{i=1}^n \left(o_{ik} \tilde{\mathbf{x}}_i \tilde{\boldsymbol{\beta}}'_k - \log(1 + e^{\tilde{\mathbf{x}}_i \tilde{\boldsymbol{\beta}}'_k}) \right) + \sum_{i=1}^n (1 - o_{ik}) (y_i \tilde{\mathbf{x}}_i \boldsymbol{\beta}'_k - e^{\tilde{\mathbf{x}}_i \boldsymbol{\beta}'_k}) + \sum_{i=1}^n (1 - o_{ik}) \log(y_i!) \\ &= l_c(\psi_k; y, \mathbf{x}, \mathbf{o}_k) + l_c(\lambda_k; y, \mathbf{x}, \mathbf{o}_k) + \sum_{i=1}^n (1 - o_{ik}) \log(y_i!) \end{aligned} \quad (3.6)$$

where \mathbf{o}_k is a realization of \mathcal{O}_k . (3.6) is easier to maximize since $l_c(\psi_k; y, \mathbf{x}, \mathbf{o}_k)$ and $l_c(\lambda_k; y, \mathbf{x}, \mathbf{o}_k)$ can be maximized separately for parameters ψ_k and λ . With the EM algorithm, the incomplete-data log-likelihood can be maximized iteratively between estimating \mathcal{O}_{ik} with its expectation under current parameters λ_k and ψ_k (E-Step) and then maximizing the complete data-loglikelihood (M-Step).

3.2.1 E-step - Zero-inflated Model

Using current estimates $\psi_k^{(s)}$ and $\lambda_k^{(s)}$ from the partition Ω_k^Z , we calculate the expected value of O_{ik} by its posterior mean $o_{ik}^{(s)}$ for each cluster k , at iteration s as

$$o_{ik}^{(s)} = \begin{cases} \left[1 + \exp(-\tilde{\mathbf{x}}_i \tilde{\boldsymbol{\beta}}'^{(s)}_k - e^{\tilde{\mathbf{x}}_i \boldsymbol{\beta}'^{(s)}_k}) \right]^{-1}, & y_i = 0 \\ 0, & y_i > 0. \end{cases}$$

3.2.2 M-Step - Zero-inflated Model

The M-Step can be split into the maximization of two complete data log-likelihoods and the \mathbf{o}_k calculated from the previous iteration (s) as

$$l_c(\lambda_k; y, \mathbf{x}, \mathbf{o}_k^{(s)}) = \sum_{i=1}^n (1 - o_{ik}^{(s)}) (y_i \tilde{\mathbf{x}}_i \boldsymbol{\beta}'_k - e^{\tilde{\mathbf{x}}_i \boldsymbol{\beta}'_k}). \quad (3.7)$$

$$l_c(\psi_k; y, \mathbf{x}, \mathbf{o}_k^{(s)}) = \sum_{i=1}^n \left(o_{ik}^{(s)} \tilde{\mathbf{x}}_i \bar{\boldsymbol{\beta}}_k' - \log \left(1 + e^{\tilde{\mathbf{x}}_i \bar{\boldsymbol{\beta}}_k'} \right) \right), \quad (3.8)$$

The maximization of (3.7) for GLM coefficients λ_k can be found by using a weighted log-linear Poisson regression with weights $1 - o_{ik}^{(s)}$ (see McCullagh and Nelder (1989)), yielding $\lambda_k^{(s+1)}$. While the parameter for (3.8) can be maximized over a gradient yielding $\psi_k^{(s+1)}$ (see Lambert (1992)).

3.3 Comparing zero-inflated Models

Until recently the usual test for comparing zero-inflated to non-zero inflated models has been the Vuong Test for non-nested models (see Vuong (1989)). However, recent work has shown the misuse of this test for zero inflation (see Wilson (2015)). Wilson and Einbeck (2018) show that it is sufficient to test for zero-modification in the form of a likelihood ratio test. The hypothesis test is defined as follows

$$H_0 : \psi_k = 0 \quad vs. \quad H_a : \psi_k \neq 0.$$

The test statistic φ defined as

$$\varphi = -2 \left[l(\tilde{\lambda}_k; y, \mathbf{x}) - l(\lambda_k, \psi_k; y, \mathbf{x}) \right]. \quad (3.9)$$

is shown to have is shown to be distributed Chi-square distrution having m degrees of freedom (χ_m^2) and confidence level $\alpha = 0.10$ (see Wilson and Einbeck (2018)). The function $l(\tilde{\lambda}_k; y, \mathbf{x})$ is the log-likelihood of a single component GCWM Poisson model on Ω_{Z_k} parameterized by $\tilde{\lambda}_k$. Recall that ψ_k is the zero-inflation paramater of the k th parition. For a more nuanced approach we will be using (3.9) to test for evidence of zero-inflation on partition Ω_k , and then using BIC for model comparisons on Ω_k . This approach quickly determines if there is zero-inflation on partition Ω_k . When evidence of zero-inflation is established, we search for the best possible linear model using BIC.

4 Numerical Application

4.1 Dataset

We illustrate the proposed methodology on the French motor severity and frequency datasets by policy. These datasets are available as part of the **R** package `CASdatasets` developed by (Dutang and Charpentier, 2016) and previously used in the book *Computational Actuarial Science with R* by Charpentier (2014). The book demonstrated various GLM modeling approaches for fitting frequency and severity of this data. Miljkovic and Fernández (2018) used the same datasets to review two mixture-based clustering approaches for modeling unobserved heterogeneity in Region 24 of this insurance portfolio. Zhang and Miljkovic (2018) introduced a Bayesian approach in ratemaking for a new territory considering also policies in French Region 24. French automobile portfolio consists of 413,169 motor third-party liability policies with the associated risk characteristics. The loss amounts by policy ID are also provided.

Table 1: The description of variables in the French Motor Third-Part Liability dataset.

Attribute	Description
Policy ID	Unique identifier of the policy holder
Claim Nb	Number of claims during exposure period (0,1,2,3,4)
Exposure	The exposure of policy in years (0–1.5)
Power	Power level of car ordered categorical (12 levels)
Car Age	Car age in years
Driver Age	Age of a legal driver
Brand	Car brands (7 types)
Gas	Diesel or Regular
Region	Regions in France (10 classifications)
Density	Number of inhabitants per km ²
Loss Amount	Portion of claim the insurance policy pays

4.2 Discussion and Results

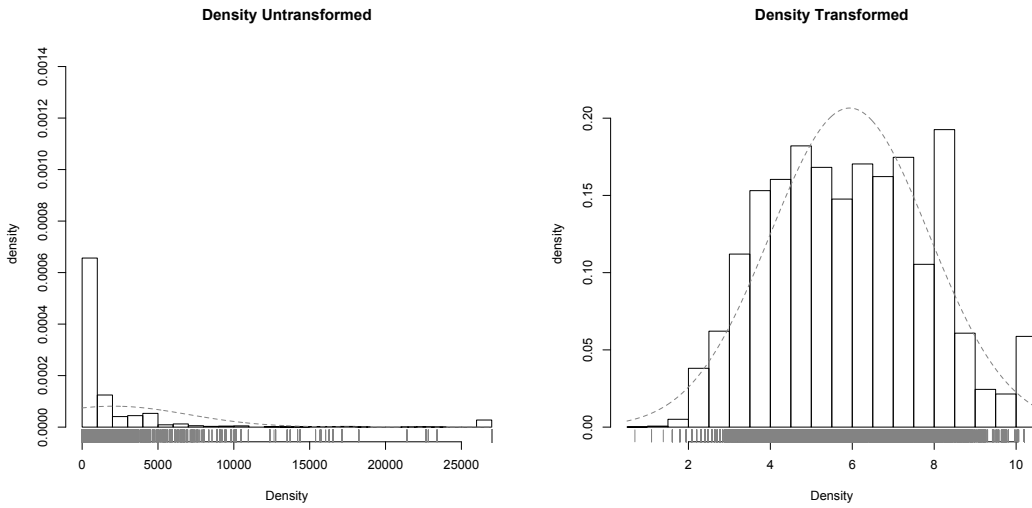
4.2.1 Modelling Severity

In this section, we show the results from modeling French motor losses. We consider the following covariates: density, driver age, car age, power, gas, and region. The model that was fitted is defined with the following equation

$$LossAmount = Density + CarAge + DriverAge + Region + Power + Gas + \epsilon, \quad \epsilon \sim \mathcal{N}(0, \sigma^2). \quad (4.1)$$

Here error term ϵ is distributed normally with mean 0 and variance σ^2 . The canonical log-link is used for the GLM in (4.1). Similarly to Miljkovic and Fernández (2018), *CarAge* is modelled as a categorical variable with five categories: $[0, 1)$, $[1, 5)$, $[5, 10)$, $[10, 15)$, and $15+$. Additionally, *DriverAge* is modelled as a categorical variable with five categories: $[18, 23)$, $[23, 27)$, $[27, 43)$, $[43, 75)$, and $75+$. *Power* is modelled into three categories as in Charpentier (2014): DEF, GH, and other.

Figure 1: Density variable: Left figure shows the fit when Gaussian distribution is imposed (CMW approach) to highly skewed data. Right figure shows the fit when log-normal assumption is applied (GCWM approach).



Beginning with the continuous covariate *Density*, we want to inspect the shape of its univariate data to see if it follows Gaussian distribution. The left side of Figure 2 clearly reveals that the *Density* is rather skewed right with several observations that report high value of density. This indicates a need for a transformation. With the log-normal assumption, the *Density* is transformed which improves the fit (see the right side of Figure 2) on the data.

The result of the transformation is a better AIC and BIC. Table 2 shows a considerable difference in BIC and AIC comparing CWM and GCWM. The five component CWM with a BIC of 285,268 is significantly higher than the four component GCWM with a considerably lower BIC of 89,568.

We now investigate the results of GCWM in relation to the valuation of risk. For practical uses, finding clusters allows us to create different classifications of risk for various groups of drivers. The following GCWM allows to cluster different drivers in groups allowing one to assign different rates to different clusters.

After fitting the model, we then inspect the size of each cluster. The GCWM approach has chosen four

Table 2: Comparison of AIC and BIC for CWM versus GCWM models.

Model	k	AIC	BIC
CWM	1	352,470	352,661
	2	314,560	314,949
	3	301,223	301,812
	4	287,020	287,808
	5	284,283	285,268
GCWM	1	111,129	111,320
	2	90,039	90,428
	3	89,476	90,065
	4	88,781	89,568
	5	88,731	89,717

Figure 2: Showing clusters by color scheme: Cluster 1 - Red, Cluster 2 - Green, Cluster 3 - Blue, Cluster 4 - Teal for *LossAmount* vs *Density* on a log scale.

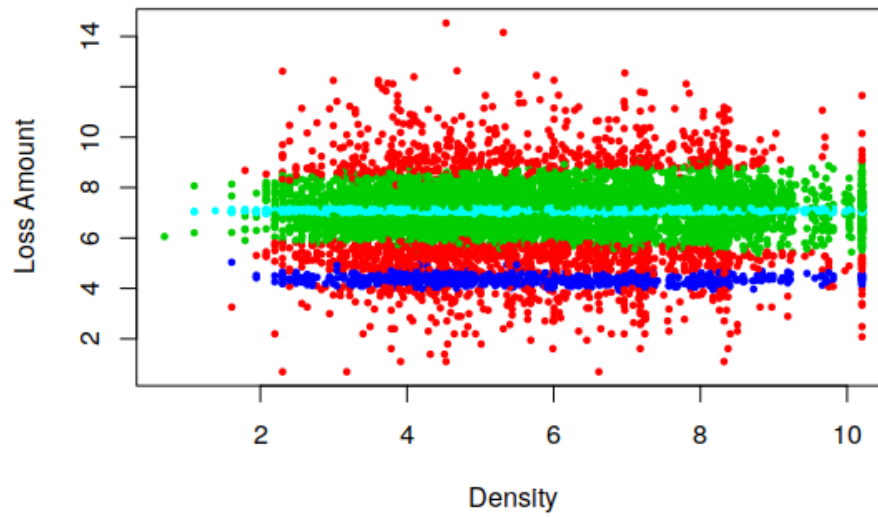


Table 3: Size of clusters for the GCWM a model.

Cluster 1	Cluster 2	Cluster 3	Cluster 4
1,683	5,766	848	7,093
Red	Green	Blue	Teal

components as the best model to represent the data. The size of each cluster is displayed in Table 3. Attention is brought to largest quantity of drivers that are grouped into Cluster 4. This accounts for 46% of all drivers and is fairly concentrated in the center of Figure 2. From the results we can create an insurance model with the

distinct characteristics.

The Cluster 3 drivers have both low variability and low average cost in claims, thus can be insured with a lower rate than other drivers. From a risk management perspective this is the most ideal case as these claims have very low variance and cost. Cluster 4 drivers have also low variability but a higher average cost, thus they would have a rate higher than Cluster 3. Cluster 2 drivers have the next highest cost and variability of the clusters, these drivers are colored in green in Figure 2. The final cluster colored in red has the highest cost and variability in claims out of any of the other clusters. From a risk management perspective this cluster would have the highest rate.

Table 4: Summarized volatility information of each cluster for Claims.

Volatility Level - (Cluster)	Minimum	Mean	Maximum	σ
V1 - (3)	51	79	154	13
V2 - (4)	1039	3109	1324	52
V3 - (2)	221	1687	8841	1284
V4 - (1)	2	9717	2036833	64835

Table 4 shows a breakdown of the types of drivers, ordered by volatility in descending order. Beginning with V1 volatility level, these drivers tend to have claims between \$51 to \$154, with a standard deviation of \$13, and a mean of \$79. That means that these drivers rarely exceed costs and tend to have very low volatility of claims. Moving onto V2, these drivers have the second lowest level of volatility. Drivers in this range tend to have claims anywhere between \$1,039 to \$3,109, with a standard deviation of \$52, and a mean of \$3,109. Proceeding to V3, it's volatility in claims is greater than the preceding levels. Drivers in this cluster have claims anywhere between \$221 to \$8841, with a mean of \$1,687, and a standard deviation of \$1284. Finally, V4 denotes the level of highest volatility. Claims in this level reach the highest recorded claim of \$2,036,833, a mean of \$97,17, and a standard deviation of \$64,835.

Coefficients of clustered results are used to calculate premiums in car insurance. Table 12 shows the coefficients of the fitted model. In each cluster statistical significance varies but overall the majority of coefficients are statistically significant.

In summary, the drivers have been clustered into four categories with distinct characteristics outlined in Table 4. We have seen how using the results from GCWM, one can create an insurance model based on clustering algorithms with various levels of risk represented in each cluster. GCWM found a group that was the clear majority of drivers, in which the volatility of their claims was extremely low regardless of *Density* or *DriverAge*. The results show that GCWM may potentially find unique clusters that are otherwise hidden within the data.

4.2.2 Modeling Claims Frequency

In this section, we model frequency of the French motor claims. We consider the covariates *Density*, *DriverAge*, *CarAge*, *Exposure* and *Power*. The choice of covariates stems from the previously modelled single component ZIP (Charpentier, 2014). The GCWM is modelled with the linear formula

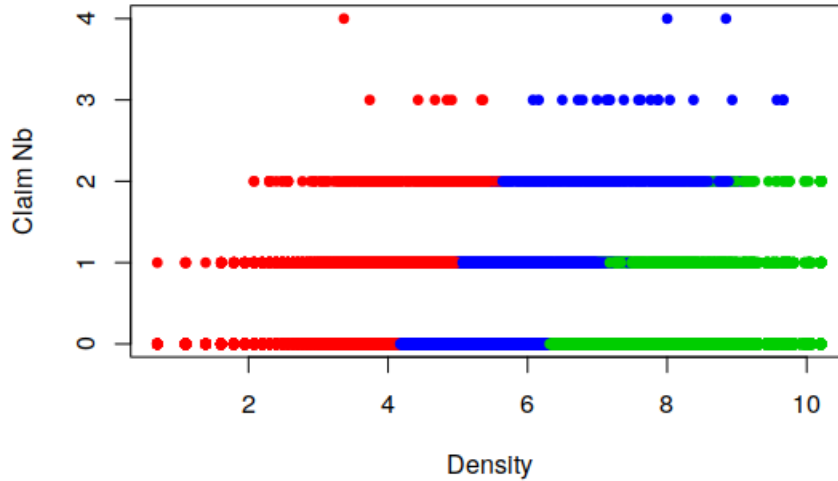
$$ClaimNb = Density + Exposure + Power \quad | \quad Exposure + CarAge \quad (4.2)$$

where *Density*, *Exposure*, and *Power* are explanatory variables in a Poisson model, while *Exposure* and *CarAge* are explanatory for a Bernoulli model. As in Section 4.2.1, we also impose a log-normal assumption on the *Density* covariate. After fitting the model, GCWM has found two zero-inflated components and one Poisson component as the best model to represent the data. The size of each cluster is displayed in Table 5. We note a fairly even spread of the size across the three clusters.

Table 5: Size of clusters for the GCWM a model.

Cluster 1	Cluster 2	Cluster 3
100492	163503	149174
Red	Green	Blue

Figure 3: Showing clusters in color for Frequency vs Density under log-normal assumptions.



Similarly to modelling severity, the GCWM finds clusters with unique characteristics. This is evident when looking at the Claims vs. Density plot in Figure 3. We see that the GCWM has split up the drivers into

three groups based on the Density of cities. Table 6 shows that Cluster 2 drivers live in the least dense cities with a mean of 7.86 km on the log scale. Followed by Clusters 3 and 1 with a mean of 5.23 km and 3.38 km respectively.

Table 6: Summary of each cluster with log-normal assumptions for the *Density* covariate measured in km on a log scale.

Cluster	Color	Minimum	Mean	Maximum	σ
1	Red	0.69	3.38	5.60	0.60
2	Green	6.29	7.86	10.20	1.03
3	Blue	4.13	5.23	9.66	0.65

Table 13 shows a summary of the coefficients for the zero-inflated model. The significance codes are the same as of Table 12. In each cluster we can see that the majority of the coefficients are significant particularly in the zero-count model for Bernoulli. Cluster 1 was selected to be strictly a Poisson model by the likelihood ratio test defined in (3.9). In summary we see that the GCWM can account for zero-inflated data in pricing.

5 Simulation Study

Two simulation studies are conducted to determine the validity of the log-normal assumption and the effectiveness of the Bernoulli-Poisson partitioning method. The first section outlines the need for a non-Gaussian assumption for the covariates. The second section shows the classification accuracy and other relevant analysis for the Bernoulli-Poisson method.

5.1 Simulation Study - GCWM

In this section, we show how the proposed methodology works for different simulation settings. The simulation study was generated based on the regression coefficients of the **CASdataset** used in the previous section. The aim of the simulation study was to test the accuracy and ability of both GCWM and CWM to return estimates of true parameters when one or more of the covariates is log-normal and the other two are Gaussian. This was designed to test both functions in the event when one of the covariates is non-Gaussian. The motivation behind this is fact is that many covariates used in insurance are likely to come from non-Gaussian distributions. Thus this was aimed to test the relevancy of CWM, which treats all covariates as Gaussian.

We define Model 1 as the base line model in which the coefficients were generated for **CASdataset** and reported in upper portion of Table 2. These coefficients were then rounded and treated as true parameters. A

simulation with three GLM mixture components was then generated around these true parameters in which the third covariate X_3 was log-normal. Stemming from this, both CWM and GCWM a were run. The GCWM a treats X_3 as a log-normal covariate.

The results for Model 1 were summarized in upper portion of Table 3 based on the performance of the GCWM a approach. The simulation was run 1000 times. We reported the percentage of runs for each predictor and the corresponding intercept in each mixture component under the assumption of 5% error. For example, predictor X_2 in the component 2 of Model 1 reported 90.10% accuracy. This means that 90.1% of the time the true parameter was estimated within 5% error. In this setting, predictor X_1 in the second component was insignificant in the real data set. The purpose of including this parameter in Model 1 was to test the sensitivity of GCWM a for insignificant predictors. In this case, the result of zero is underlined and it means that it has no influence on the response variable in this simulation. Further, we created Models 2, 3, 4 and 5 by altering the parameters of Model 1 by +30%, -30%, +50%, and -50% accordingly and keeping the second covariate of the second component as an insignificant predictor from the **CASdataset** model. This was done to test the accuracy of GCWM a to the sensitivity of coefficients. Based on the results in Table 7, we can see that GCWM performs well for all simulation settings.

Table 7: GCWM a vs CWM Accuracy: covariate X_3 is treated as log-normally distributed, while the rest of covariates are of the Gaussian type.

Model	Component	Intercept	X_1	X_2	X_3	Intercept	X_1	X_2	X_3
1	1	93.00%	90.10%	93.00%	93.10%	0.00%	0.00%	0.00%	0.00%
	2	90.10%	<u>0.00%</u>	90.10%	90.10%	0.00%	0.00%	0.00%	0.00%
	3	99.20%	99.10%	99.20%	99.20%	0.00%	0.00%	0.00%	0.00%
2	1	89.80%	89.20%	89.80%	89.80%	0.00%	0.00%	4.60%	0.00%
	2	89.20%	<u>0.00%</u>	89.20%	89.20%	0.00%	<u>0.00%</u>	0.00%	0.00%
	3	99.20%	99.20%	99.20%	99.20%	0.00%	0.20%	1.70%	0.00%
3	1	100.00%	100.00%	100.00%	100.00%	0.00%	0.00%	0.00%	0.00%
	2	100.00%	<u>0.00%</u>	100.00%	100.00%	0.00%	0.00%	0.00%	0.00%
	3	99.20%	99.20%	99.20%	99.20%	0.00%	0.00%	0.00%	0.00%
4	1	88.60%	86.80%	88.60%	87.00%	0.00%	0.00%	0.00%	0.00%
	2	86.90%	<u>0.00%</u>	86.90%	86.90%	0.00%	<u>0.00%</u>	0.00%	0.00%
	3	99.20%	99.20%	99.20%	99.20%	0.00%	0.00%	0.00%	0.00%
5	1	85.90%	84.90%	85.60%	85.90%	0.00%	0.00%	0.00%	0.00%
	2	85.00%	<u>0.00%</u>	84.90%	84.90%	0.00%	<u>0.00%</u>	0.00%	0.00%
	3	99.20%	99.20%	99.20%	99.20%	0.00%	0.20%	10.90%	0.00%

In line with expectations we note that barely any of the simulation runs are estimated correctly, as most

of the results are zero. This means that the performance of CWM approach is poor in presence of one non-Gaussian covariate which in this case is a log-normal covariate.

Table 8 provides the summary of Mean Squared Errors¹ (MSE) of each parameter of the models for the same simulated runs in Table 7.

Table 8: GCWM results: the summary of MSE for all parameters used in five models. The covariate X_3 is treated as log-normal distributed, while the rest of covariates are Gaussian. These results correspond to same simulated runs as those in Table 7.

Model	Component	β_o	MSE(β_o)	β_1	MSE(β_1)	β_2	MSE(β_2)	β_3	MSE(β_3)
1	1	1028	(11.353)	0.03	(0.00)	3.5	(0.00)	-380	(0.09)
	2	1600	(0.000)	-0.01	(0.00)	1.5	(0.00)	-250	(0.00)
	3	40000	(0.035)	-6.00	(0.00)	-305	(0.00)	1100	(0.47)
2	1	1350	(0.167)	0.04	(0.00)	4.5	(0.00)	-500	(0.03)
	2	2080	(0.001)	0.04	(0.00)	2.0	(0.00)	-325	(0.00)
	3	52000	(0.012)	-8.00	(0.00)	450	(0.00)	14300	(0.01)
3	1	720	(0.001)	0.02	(0.00)	2.5	(0.00)	-266	(0.00)
	2	1100	(0.008)	0.00	(0.00)	1.1	(0.00)	-17511	(0.00)
	3	28000	(0.002)	-4.20	(0.00)	245	(0.00)	7700.	(0.00)
4	1	1650	(13.056)	0.05	(0.00)	5.3	(0.00)	-570	(0.00)
	2	2400	(0.000)	-0.01	(0.00)	2.3	(0.00)	-375	(0.00)
	3	60000	(0.051)	-9.00	(0.00)	-457	(0.00)	16500	(0.00)
5	1	500	(1.115)	0.02	(0.00)	2.0	(0.00)	-190	(0.05)
	2	800	(0.003)	0.00	(0.00)	0.8	(0.00)	-120	(0.00)
	3	20000	(0.000)	-3.00	(0.00)	-150	(0.00)	5500	(0.00)

The MSEs related to the predictor variables for all models and their corresponding components are about zero indicating that GCWM a approach performs well. This is also a result of having a small size coefficients.

In contrary to the results reported in Table 5, these results in Table 6 are significantly different. We can observe that the MSEs for most of the Models and their corresponding coefficients are not calculated at all due to convergence failures and as such they are shown as (\cdot). This is not surprising because Table 4 shows the accuracy of CWM is not good when attempting to model non-Gaussian predictors as Gaussian.

In summary, our simulation results showed good performance of the GCWM approach in modeling non-Gaussian covariates. More specifically, these results show high accuracy when covariates are log-normal. In contrary, CWM fails to estimate parameters accurately when the Gaussian assumption is violated.

¹The MSE is computed using the following formula $MSE(\beta) = \frac{\sum_i^n (\beta_i - \hat{\beta}_i)^2}{n}$. Here, n accounts for the number of simulation runs, β is the true parameter of interest, while $\hat{\beta}$ accounts for its estimate

Table 9: CWM results: the summary of MSE for all parameters used in five models. All three covariates are treated as Gaussian. These results correspond to those in Table 4.

Model	Component	β_o	MSE(β_o)	β_1	MSE(β_1)	β_2	MSE(β_2)	β_3	MSE(β_3)
1	1	1028	(\cdot)	0.03	(\cdot)	3.5	(\cdot)	-380	(\cdot)
	2	1600	(\cdot)	-0.01	(\cdot)	1.5	(\cdot)	-250	(\cdot)
	3	40000	(\cdot)	-6.00	(\cdot)	-305	(\cdot)	1100	(\cdot)
2	1	1350	(\cdot)	0.04	(\cdot)	4.5	(\cdot)	-500	(\cdot)
	2	2080	(\cdot)	0.04	(\cdot)	2.0	(\cdot)	-325	(\cdot)
	3	52000	(\cdot)	-8.00	(0.006)	450	(44.1)	14300	(\cdot)
3	1	720	(\cdot)	0.02	(\cdot)	2.5	(\cdot)	-266	(\cdot)
	2	1100	(65.814)	0.00	(\cdot)	1.1	(\cdot)	-17511	(\cdot)
	3	28000	(\cdot)	-4.20	(\cdot)	245	(\cdot)	7700.	(\cdot)
4	1	1650	(\cdot)	0.05	(\cdot)	5.3	(\cdot)	-570	(\cdot)
	2	2400	(\cdot)	-0.01	(\cdot)	2.3	(\cdot)	-375	(\cdot)
	3	60000	(\cdot)	-9.00	(\cdot)	-457	(\cdot)	16500	(\cdot)
5	1	500	(\cdot)	0.02	(\cdot)	2.0	(\cdot)	-190	(\cdot)
	2	800	(\cdot)	0.00	(\cdot)	0.8	(\cdot)	-120	(\cdot)
	3	20000	(\cdot)	-3.00	(0.003)	-150	(4.7)	5500	(\cdot)

5.2 Simulation Study - Bernoulli-Poisson Partitioning

In this section we show how the Bernoulli-Poisson (BP) partitioning method behaves under different conditions. The components were generated under similar coefficients taken from the **CASDatasets** package. The coefficients were rounded and treated as true parameters to which data was generated from. The mean and standard deviation of the covariates within each component was also taken into account when generating data. The first simulation examines the performance of the GCWM model for classification. We generate three components each with sample size $N = 1000$ for a total of 3000 simulated points. The model generated is similar to the mean and standard deviations of Table 6. Consider three simulated covariates and

$$SimClaimsNb = SimDriverAge + SimDensity + SimCarAge \quad (5.1)$$

as the GLM. The covariates *SimDriverAge*, *SimDensity*, and *SimCarAge* are considered for both the Poisson and Bernoulli models. Here the GCWM is fitted to the simulated data and used to classify into three components. The misclassification rate is calculated by the proportion of true labels placed in other components by the GCWM a model. The results of the simulation is based on the generated dataset are presented in Table 10. The total misclassification rate is 1.8% and the majority of misclassified components are between components two and three.

The experiment is expanded further to show how Bernoulli-Poisson partitioning behaves over 1000 runs

Table 10: Misclassification rate and label comparison of generated data.

True Labels	Classified			Misclassification Rate
	1	2	3	
1	992	3	5	0.80 %
2	0	990	10	1.00 %
3	15	20	965	3.50 %
Overall Misclassification Rate				1.80 %
Average Purity				98.23 %
Adjusted Rand Index				0.9479

and under two different conditions. The first condition is defined as follows. The mean and standard deviations are taken as given by the estimated ZIP components from the **CASDataset**. The second condition involves adjusting the means of two of the covariates so they are closer to each other. The goal is to show that the BP-method holds its use even when means among covariates are close. The conditions are divided into two scenarios. In the first scenario which we consider “normal”, the covariate means are taken directly from the sample data. In the second scenario “close” as the covariate means are manipulated so that they are closer to each other within some degree. This is a common problem in classification where if the means among two different components are close, then misclassification rate increases (Lim et al., 2014). Experiment 2 tests the accuracy of 3 different partitioning methods to initialize a zero-inflated model. The Poisson partitioning method assumes that the presence of non-zeros will provide a better partitioning of the data-set. The Bernoulli partitioning method assumes that the presence of excess zeros will determine the best partitioning of the data-set. Finally the BP partitioning method assumes that both methods are weighed equally and therefore both must be taken into account when partitioning the dataset. The mean and standard deviation of each measurement is provided in Table 11.

Table 11: Experiment 2: mean and standard deviations for each statistic compared across methods.

Type	Condition	Poisson	(σ)	Bernoulli	(σ)	BP	(σ)
Misclassification Rate	normal	1.70%	(6.00)	1.60%	(6.00)	1.10%	(0.02)
	close	5.00%	(7.00)	6.00%	(2.00)	7.00%	(4.00)
Average Purity	normal	98.87%	(2.00)	98.91%	(2.25)	99.18%	(0.81)
	close	95.38%	(4.00)	94.55%	(1.00)	96.95%	(0.48)
Adjusted Rand Index	normal	0.9662	(0.07)	0.9677	(0.07)	0.9729	(0.0217)
	close	0.8706	(0.08)	0.8366	(0.04)	0.8538	(0.0453)

Several findings are concluded from Table 11. Under condition normal, the BP method shows better

performance in error and is found to be less sensitive than other methods with an error rate of 1.10% and a standard deviation of 0.02%. Further findings show that when close condition is imposed then Bernoulli has better performance in terms of accuracy. The Adjusted Rand Index² (ARI) shows good measurements overall, but in particular the BP partitioning method under normal scenario has a very good ARI with a small standard deviation. The Average Purity³ (AP) of the BP partitioning method is the best out of all other methods, which is relevant to estimating coefficients accurately for optimization.

6 Conclusion

In this paper, we extend the class of generalized linear mixture CWM models by accomplishing two main goals. First, we proposed the methodology that allows for continuous covariates to follow a non-Gaussian distribution. Imposing Gaussian distribution on a skewed data may result in an suboptimal model fit. Second, we proposed a new Poisson CWM methodology that uses Bernoulli-Poisson partitioning method and allows for implementation of zero-inflated Poisson CWM model (ZI-GCWM). We name our proposed model class as the Generalized Cluster-Weighted Model (GCWM), to reflect the two extensions made to the existing CWM class of models.

Our proposed GCWM models allow for great applications in predictive modeling of insurance claims by overcoming a few limitations of the current CWM models. The ZI-GCWM allows for finding clusters within claims frequency which is an important information in risk classification and modeling of claims frequency. Further, some insurance rating variables used in the predictive modeling of severity claims may not strictly follow Gaussian assumptions, for example driver's age or car age, when treated as continuous covariates. An adequate extension to non-Gaussian covariates can be considered to relax current assumptions and improve the model fit. Given our data, we convincingly demonstrated that there is a need for a log-normal assumption in the *Density* covariate, and by making it we have consideredly the model fit.

The results of our extensive simulation study showed the excellent performance of the proposed models in case of modeling non-Gaussian covariates. We found that current CWM model fails to estimate the parameters accurately when the Gaussian assumption is violated. The GCWM shows significant improvement in the model fit over the CWM model based on AIC and BIC criteria. We also tested Bernoulli-Poisson partitioning of zero-inflated GCWM under different conditions and found that our proposed partitioning method has a very

²The adjusted rand index is calculated as $ARI = \frac{\sum_{ij} \binom{n_{ij}}{2} - [\sum_i \binom{a_i}{2} \sum_j \binom{b_j}{2}] / \binom{n}{2}}{\frac{1}{2} [\sum_i \binom{a_i}{2} + \sum_j \binom{b_j}{2}] - [\sum_i \binom{a_i}{2} \sum_j \binom{b_j}{2}] / \binom{n}{2}}$

³ $AP = \frac{1}{N} \sum_i n_{ij}$,
where n_{ij} = across diagonal, a_i = row sums, b_j = column sums are of the classification matrix in Table 10.

low misclassification rate, high average purity, and high average rand index.

Our approach is relevant to the actuarial pricing and risk management when current practices are based on implementation of various GLM models. Further extension of this work may incorporate modifications of the CWM family to allow for modeling limited depended variable or the right-censored data structure (refer to Miljkovic and Barabanov (2015) and Miljkovic and Orr (2017)).

7 Appendix

7.1 Derivation of the Log-normal Distribution

Consider a random variable U having univariate log-normal distribution with parameters $\mu \in \mathbb{R}$ and $\sigma \in \mathbb{R}_+$.

Have $u \in \mathbb{R}_+$, then the probability density function of random variable U is defined as ⁴

$$\mathcal{LN}(u; \mu, \sigma) = \frac{1}{u\sigma\sqrt{2\pi}} \exp \left[-\frac{(\ln u - \mu)^2}{2\sigma^2} \right].$$

Further, if random variable X is normally distributed i.e. $X \sim \mathcal{N}(x; \mu, \sigma)$, then $U := \exp(X) \sim \mathcal{LN}(u; \mu, \sigma)$.

To see this, let $p_U(u)$, and $p_X(x)$ be the probability density functions of U and X respectively. By the change of variables theorem (see Murphy and Bach (2012) section 2.6.2.1) the density $p_U(u)$ is derived as

$$p_U(u) = p_X(\ln u) \frac{\partial}{\partial u} \ln u = p_X(\ln u) \frac{1}{u} = \frac{1}{u\sigma\sqrt{2\pi}} \exp \left[-\frac{(\ln u - \mu)^2}{2\sigma^2} \right].$$

We extend to a log-normal multivariate case where the random variable \mathbf{U} is parameterized by $\boldsymbol{\mu} \in \mathbb{R}^p$ and $\boldsymbol{\Sigma} \in \mathbb{R}_+^p$.

Lemma 7.1. *Let the random variable \mathbf{X} have multivariate normal distribution ie. $\mathbf{X} \sim \mathcal{MVN}(\mathbf{x}, \boldsymbol{\mu}, \boldsymbol{\Sigma})$, then $\mathbf{U} := \exp(\mathbf{X}) \sim f^U(\mathbf{u}; \boldsymbol{\mu}, \boldsymbol{\Sigma})$. Here have $\mathbf{u} \in \mathbb{R}_+^p$ and the probability density function f^U is*

$$f^U(\mathbf{u}; \boldsymbol{\mu}, \boldsymbol{\Sigma}) = \frac{1}{(\prod_{i=1}^p u_i) |\boldsymbol{\Sigma}| (2\pi)^{\frac{p}{2}}} \exp \left[-\frac{1}{2} (\ln \mathbf{u} - \boldsymbol{\mu})' \boldsymbol{\Sigma}^{-1} (\ln \mathbf{u} - \boldsymbol{\mu}) \right].$$

Proof. Let $f^U(\mathbf{u}; \boldsymbol{\mu}, \boldsymbol{\Sigma})$ and $f^X(\mathbf{x}; \boldsymbol{\mu}, \boldsymbol{\Sigma})$ be the probability density functions of \mathbf{U} and \mathbf{X} respectively. By the multivariate change of variables theorem (see Murphy and Bach (2012) section 2.6.2.1), we derive the log-normal distribution, where $|\det J_{\ln}(\mathbf{u})|$ is the absolute value of the determinant for the Jacobian of the multivariate transformation $\ln(\mathbf{U}) = \mathbf{X}$. Hence,

$$\begin{aligned} |\det J_{\ln}(\mathbf{u})| &= \prod_{i=1}^p u_i^{-1}, \text{ and} \\ f^U(\mathbf{u}; \boldsymbol{\mu}, \boldsymbol{\Sigma}) &= f^X(\ln \mathbf{u}; \boldsymbol{\mu}, \boldsymbol{\Sigma}) |\det J_{\ln}(\mathbf{u})| \\ &= f^X(\ln \mathbf{u}; \boldsymbol{\mu}, \boldsymbol{\Sigma}) \prod_{i=1}^p u_i^{-1} \\ &= \frac{1}{(\prod_{i=1}^p u_i) |\boldsymbol{\Sigma}| (2\pi)^{\frac{p}{2}}} \exp \left[-\frac{1}{2} (\ln \mathbf{u} - \boldsymbol{\mu})' \boldsymbol{\Sigma}^{-1} (\ln \mathbf{u} - \boldsymbol{\mu}) \right]. \end{aligned}$$

□

⁴For full definition see Johnson et al. (1995)

Table 12: Summary of coefficients for severity clusters.

Coef	V1 (Red)		V2 (Green)		V3 (Blue)		V4 (Teal)	
	Estimate	Error	P	Estimate	Error	P	Estimate	Error
Intercept	7.876	0.137	***	7.180	0.061	***	4.673	0.014
Density	-0.031	0.009	***	0.005	0.004	***	-0.011	0.001
C2	-0.172	0.080	*	0.064	0.034	.	0.020	0.001
C3	-0.396	0.080	***	0.108	0.034	**	0.010	0.007
C4	-0.642	0.081	***	-0.033	0.035	***	0.034	0.007
C5	-0.500	0.090	***	0.066	0.039	.	0.069	0.007
D2	-0.535	0.083	***	-0.168	0.038	***	-0.217	0.009
D3	-0.607	0.084	***	-0.241	0.038	***	-0.205	0.009
D4	-0.390	0.099	***	-0.122	0.045	**	-0.200	0.0106
D5	0.123	0.101		0.035	0.047		-0.138	0.010
R23	0.003	0.131		-0.016	0.053		-0.001	0.012
R24	-0.232	0.054	***	-0.017	0.023		-0.102	0.005
R25	0.144	0.096		-0.184	0.043	***	-0.065	0.009
R31	-0.009	0.073		0.055	0.031	.	-0.141	0.008
R52	-0.303	0.064	***	0.012	0.028		-0.142	0.006
F53	-0.153	0.063	*	0.095	0.028	***	-0.012	0.006
R54	-0.222	0.082	**	0.074	0.037	*	-0.122	0.007
R72	-0.098	0.072		0.175	0.031	***	-0.081	0.007
R74	-0.236	0.142	.	-0.114	0.067	.	0.466	0.016
P-FGH	0.123	0.033	***	0.012	0.015		0.001	0.003
P-Other	0.131	0.045	**	0.075	0.020	***	0.012	0.003
GR	-0.095	0.031	**	-0.029	0.014	*	0.005	0.002

^aThe significance codes are defined as $P < 0.001$: (***), $0.001 < P < 0.01$: (**), $0.01 < P < 0.05$: (*), $0.05 < P < 0.10$: (.) pertaining to the P value of the specific coefficient.

Table 13: Summary of coefficients for frequency clusters.

Coef	Cluster 1 (Red)			Cluster 2 (Green)			Cluster 3 (Blue)		
	Estimate	Error	P	Estimate	Error	P	Estimate	Error	P
(Intercept)	-10.199	0.109	***	-7.217	0.216	***	-13.694	0.099	***
Density	1.860	0.027	***	0.442	0.013	***	1.771	0.013	***
Exposure	0.825	0.040	***	0.726	0.192	***	0.745	0.046	***
P-GH	-0.063	0.030	*	-0.004	0.035		0.013	0.030	
P-Other	-0.019	0.042		0.049	0.043		0.107	0.040	**
(Intercept)				2.424	0.188	***	1.886	0.356	***
Exposure				-5.871	0.758	***	16.520	2.990	***
C2				-0.541	0.176	**	-0.922	0.368	*
C3				-1.217	0.201	***	-2.263	0.553	***
C4				-1.265	0.225	***	10.805	72.677	
C5				-0.808	0.266	**	-6.355	30.867	

^aThe significance codes are defined as $P < 0.001$: (***), $0.001 < P < 0.01$: (**), $0.01 < P < 0.05$: (*), $0.05 < P < 0.10$: (.) pertaining to the P value of the specific coefficient.

References

- Bermúdez, L., Karlis, D., 2012. A finite mixture of bivariate poisson regression models with an application to insurance ratemaking. *Computational Statistics and Data Analysis* 56 (12), 3988–3999.
- Biernacki, C., Celeux, G., Govaert, G., Jul 2000. Assessing a mixture model for clustering with the integrated completed likelihood. *IEEE Transactions on Pattern Analysis and Machine Intelligence* 22 (7), 719–725.
- Brown, G., Buckley, W., 2015. Experience rating with poisson mixtures. *Annals of Actuarial Science* 9 (02), 304–321.
- Charpentier, A., 2014. *Computational Actuarial Science with R*. CRC press.
- Dempster, A. P., Laird, N. M., Rubin, D. B., 1977. Maximum likelihood from incomplete data via the EM-algorithm. *Journal of the Royal Statistical Society B* 39, 1–38.
- Durham, G. B., 2007. Sv mixture models with application to s&p 500 index returns. *Journal of Financial Economics* 85 (3), 822–856.
- Dutang, C., Charpentier, A., 2016. *CASdatasets*. R package version 1.0-6.
URL <http://cas.uqam.ca/pub/R/>
- Gershensfeld, N., 1997. Nonlinear inference and cluster-weighted modeling. *Annals of the New York Academy of Sciences* 808 (1), 18–24.
- Gershensfeld, N., 1999. *The nature of mathematical modeling*. Cambridge university press.
- Gershensfeld, N., S. B., Metois, E., ., 1999. Cluster-weighted modelling for time-series analysis. *Nature* 397 (67171), 329–332.
- Ingrassia, S., M. S., Punzo, A., 2014. Model-based clustering via linear cluster-weighted models. *Computational Statistics & Data Analysis* 71, 159–182.
- Ingrassia, S., M. S., Vittadini, G., 2014. Local statistical modeling via a cluster-weighted approach with elliptical distributions. *Journal of classification* 29 (3), 363–401.

- Ingrassia, S., P. A. V. G., Minotti, S., 2015. The generalized linear mixed cluster-weighted model. *Journal of Classification* 32 (1), 85–113.
- Johnson, N., Kotz, S., Balakrishnan, N., 1995. Continuous univariate distributions. No. v. 2 in *Wiley series in probability and mathematical statistics: Applied probability and statistics*. Wiley & Sons.
URL <https://books.google.ca/books?id=0QzvAAAAMAAJ>
- Lambert, D., 02 1992. Zero-inflated poisson regression, with an application to defects in manufacturing 34, 1–14.
- Lee, S. C. K., Lin, X. S., 2010. Modeling and evaluating insurance losses via mixtures of Erlang distributions. *North American Actuarial Journal* 14 (1), 107–130.
- Lim, H., Li, W., Yu, P., 03 2014. Zero-inflated poisson regression mixture model 71, 151–158.
- McCullagh, P., Nelder, J., 1989. *Generalized linear models*. Vol. 37. CRC press.
- McLachlan, S., Peel, D., 2000. *Finite Mixture Models*. John Wiley & Sons, Hoboken, NJ.
- McNicholas, P., Murphy, T., McDaid, A., Frost, D., 2010. Serial and parallel implementations of model-based clustering via parsimonious gaussian mixture models. *Computational Statistics Data Analysis* 54 (3), 711 – 723, second Special Issue on Statistical Algorithms and Software.
URL <http://www.sciencedirect.com/science/article/pii/S0167947309000632>
- Miljkovic, T., Barabanov, N., 2015. Modeling veterans health benefit grants using the expectation maximization algorithm. *Journal of Applied Statistics* 42 (6), 1166–1182.
- Miljkovic, T., Fernández, D., May 2018. On two mixture-based clustering approaches used in modeling an insurance portfolio. *Risks* 6 (2), 57.
URL <http://dx.doi.org/10.3390/risks6020057>
- Miljkovic, T., Grün, B., 2016. Modeling loss data using mixtures of distributions. *Insurance: Mathematics and Economics*.
- Miljkovic, T., Orr, M., 2017. An evaluation of the reconstructed coefficient of determination and potential adjustments. *Communications in Statistics-Simulation and Computation* 46 (9), 6705–6718.
- Miljkovic, T., SenGupta, I., 2018. A new analysis of vix using mixture of regressions: Examination and short-term forecasting for the s & p 500 market. *High Frequency* 1 (1), 53–65.

Murphy, K., Bach, F., 2012. Machine Learning: A Probabilistic Perspective. Adaptive Computation and Machi. MIT Press.

URL <https://books.google.ca/books?id=NZP6AQAAQBAJ>

Punzo, A., Ingrassia, S., ., 2014. Parsimonious generalized linear Gaussian cluster-weighted models. Springer International Publishing.

Verbelen, R., Gong, L., Antonio, K., Badescu, A., Lin, S., 2015. Fitting mixtures of Erlangs to censored and truncated data using the EM algorithm. ASTIN Bulletin 45 (3), 729–758.

Vuong, Q. H., 1989. Likelihood ratio tests for model selection and non-nested hypotheses. Econometrica 57 (2), 307–333.

URL <http://www.jstor.org/stable/1912557>

Wedel, M., 2002. Concominat variables in finite mixture modeling. Statistica Neerlandica 56 (3), 362–375.

Wedel, M., De Sabro, W., 1995. A mixture likelihood approach for generalized linear models. Journal of Classification 12 (3), 21–55.

Wilson, P., 02 2015. The misuse of the vuong test for non-nested models to test for zero-inflation 127.

Wilson, P., Einbeck, J., 2018. A new and intuitive test for zero modification. Statistical Modelling.

URL <http://hdl.handle.net/2436/621356>

Zhang, J., Miljkovic, T., 2018. Ratemaking for a new territory: Enhancing glm pricing model with a bayesian analysis. E-Forum 2 (6), 1–33.

URL <https://www.casact.org/pubs/forum/18spforumv2/CompleteSpring2018Volume2.pdf>